

MODELING OF WATER WETTING IN OIL-WATER PIPE FLOW

Jiyong Cai and Srdjan Nesic
Institute for Corrosion and Multiphase Technology
Ohio University
342 W.State St, Athens, OH 45701

Cornelis de Waard
CorCon Consultancy
Generaal Winkelmanlaan 77
2111 WV Aerdenhout, Netherlands

ABSTRACT

Internal CO₂ corrosion in crude oil transport pipelines is always associated with the presence of “free” water, and the likelihood of corrosion generally increases with the volume fraction of the water phase. A recently developed method is applied here to predict the critical velocity for entraining the water by the flowing oil phase. Entrainment of the water eventually eliminates the corrosion problem. The effects of pipe diameter, surface tension, oil viscosity and density on the critical velocity for water entrainment are discussed in detail in this paper.

On the other side, if all the water is not entrained by the flowing oil phase, it is important to predict the thickness of the water film, the in-situ: water cut, film velocity and wetted area. A new model is proposed here that can be used to calculate these parameters, which are crucial for corrosion prediction in multiphase flow. A comparison is carried out between this new model and experiments conducted in large diameter horizontal pipe flow.

Keywords: modeling, water entrainment, water wetting, critical velocity, oil-water flows, three-layer model

INTRODUCTION

The simultaneous flow of oil and water in crude oil production and transportation pipelines is a common occurrence, seen anywhere from the well perforations to the final stages of separation. Carbon dioxide is also commonly present and dissolves in the water phase to form carbonic acid. At low water cuts this is not an issue as water-in-oil dispersion are observed i.e. all the water is entrained by the flowing oil. As the water cut increases, water “break-out” may occur, leading to stratified flow of separate layers of water and oil phases. Therefore, the possibility of corrosion is very high where the water phase wets the pipe wall (typically at the bottom).

It has been commonly accepted that the likelihood of corrosion generally increases with the volume fraction of water, i.e. water cut. Other factors, which are recognized as being important, are the steel composition, water chemistry and the flowing conditions. In the past, the effect of flow has been considered only in a qualitative sense. Highly turbulent flow was associated with negligible corrosion, whereas low flow rates or intermittent flow has been associated with corrosion conditions. Hence, it is a challenge for corrosion engineers to determine more precisely the flow conditions leading to corrosion and conversely the conditions leading to entrainment of the free water layer by the flowing oil phase.

Little research has been performed in the past on this subject. Wicks and Fraser (1975)¹ proposed a simplified model for predicting the critical velocity of the flowing oil phase needed to sweep out settled water. This model was based on two essential premises: (1) once entrained in the flowing oil, the water droplets behave like solid particles; (2) the lower limit of velocity sustaining net axial transport of droplets is equal to the upper limit of velocity for existence of a stratified layer. They pointed out the mechanism of entrainment: fast moving oil flowing over the free water layer causes water waves to form. Increasing oil velocity leads to unstable conditions for the water waves. Water droplets are torn off from the crests of water waves. If the velocity of oil phase is high enough, water droplets will be entrained in the oil phase and eventually all water phase will be swept away. The oil and water specific gravities, the interfacial tension between oil and water phase, the viscosity of oil phase, pipe diameter and velocity have significant effects on the water entrainment. However, the Wicks and Fraser¹ model is suitable primarily for very low water cut situations. At high water cut, their model underestimates the critical velocity without considering the coalescence of water droplets. Wu² (1995) modified Wicks and Fraser¹ model without a big improvement in the performance.

In 1987, Smith et al.³ published data that show the ability of some oils to carry water up to a 20% water cut, if flowing at velocities larger than 1 m/s. In the CO₂ corrosion model of de Waard and Lotz⁴ published in 1993, the presence of the hydrocarbon phase was accounted through a so-called water-wetting factor. From the original experiments of Wicks and Fraser¹ a binary prediction factor was extracted suggesting that oil-wetting will occur only for water cuts less than 30% and velocities larger than 1 m/s, when all water can be entrained in the oil phase. In another study published the same year (1993), Adams et al.⁵ estimated that below 30% water cut the tubing will be oil-wet; from 30-50%, intermittent water wetting occurs, and over 50% the tubing is water wet. These are very crude criteria that neglect or oversimplify the varying properties of the oil and water phases, the flow regime and the flow geometry. Furthermore, field experience suggests that in some cases corrosion was obtained at water cuts as low as 2%, in others no corrosion was obtained for water cuts as high as 50%.

C. de Waard et al.⁶ in 2001 and 2003 updated the original de Waard and Lotz⁴ empirical model from 1993 and proposed a new empirical model using an analysis based on the emulsion breakpoint approach. A link between API gravity, emulsion stability and water wetting of steel by an oil-water

mixture was considered by taking into account the changes in interfacial tensions in an oil-water-steel system. This was a major step forward from the original model, however, while agreeing reasonably well with the specific pool of field cases used for its calibration, the new model remains an empirical correlation built on limited field data with an uncertain potential for extrapolation. More importantly, this model does not consider the effect of pipe diameter, oil density, oil viscosity and system temperature on the critical velocity of the flowing oil phase required for entrainment.

To understand the mechanism of water entrainment in the oil-water pipe flows, it is necessary to look closer into different flow regimes that occur. The main difficulties in understanding and modeling of the behavior of oil-water flows arise from the existence of interfaces between the phases. The internal structures of two-phase flow can be best described by the flow patterns. The momentum and mass transfer mechanisms between the two phases significantly depends on the flow patterns. Also, flow patterns can indicate the phase wetting the pipe wall, position of the phases and the degree of mixing during the flow. Compared to gas-liquid flow studies, a much more limited number of studies⁷⁻²² are dedicated to flow of two immiscible liquids such as water and oil. Nevertheless, there is enough understanding of the flow dynamics to give us an opportunity to formulate a model that goes beyond the excellent effort of Wicks and Fraser¹.

Various flow patterns observed in the horizontal pipe flows are given in the FIGURE 1. Stratified flow with a complete separation of water and oil phases may exist at very low flow rates. With increasing the flow rate, the interface displays a wavy character with possible entrainment of droplets at one side or both sides of the interface (semi-stratified flow). The entrainment processes for both phases increase with the flow rates. When the pure water and oil layers are still continuous at the bottom and top of the pipe respectively, and a layer of dispersed droplets exists at the interface, a three-layer structure is formed. At sufficiently high oil flow rate and low water cut, the entire water phase becomes discontinuous in a continuous oil phase resulting in a water-in-oil dispersion. Vice versa, at sufficiently high water flow rate and a high water cut, the entire oil phase becomes discontinuous in a continuous water phase resulting in an oil-in-water dispersion.

In this paper, we will focus initially on formulating a criterion for predicting water entrainment, i.e. the dispersed water-in-oil flow pattern. A stable water-in-oil dispersion is characterized by no free water layer existing in the pipeline, i.e. it is the case when there is no corrosion risk. Subsequently we will address the other case when free water exists i.e. the stratified and semi-stratified flow regimes. Prediction of corrosion rates under these flow conditions requires knowledge of in-situ water cut, water velocity, water film thickness and water wetted pipe area. In this paper, a new model will be proposed to calculate the in-situ water, water velocity, the thickness of water film and water wetted pipe wall area in oil-water pipe flows.

THE MODEL

Water Entrainment

A new approach following Brauner²³ and Barnea²⁵ for predicting water-in-oil fully dispersed flow will be discussed below. A criterion for forming stable water-in-oil dispersed flow will be derived as the means of calculating the critical velocity for water entrainment. Two main physical properties, *maximum droplet size* related to breakup and coalescence and *critical droplet size* related to settling and separation, will be compared to deduce this criterion.

Maximum Droplet Size

Since water is entrained by the flowing oil phase in the form of fine droplets, it is essential to know the maximum droplet size that can be sustained by the flow without further breakup. Hinze²⁴ (1955) employed dimensional analysis to examine the forces controlling the breakup of a liquid droplet in the continuum of another liquid. He concluded that the dynamic pressure force of the turbulent motions is the factor determining the size of the largest droplets. Deformation or breakup occurs if the dynamic pressure force, caused by changes in velocity over a distance approximating the diameter of the droplet, is bigger than the counteracting interfacial tension force. He argued that the splitting of a drop in turbulent flow depends on the critical *Weber number* (We_{crit}),

$$We_{crit} = \frac{\tau d_{max}}{\sigma} \quad (1)$$

which represents the ratio between the external hydrodynamic stresses (τ) that tend to deform the drop, and the counteracting surface tension σ . Hinze's mechanism for breakage of droplets in the turbulent flow was used for predicting transition to fully dispersed flow patterns in liquid-liquid flows (Brauner²³). Two separate cases can be distinguished here: *dilute water-in-oil dispersions* and *dense water-in-oil dispersions* according to the mechanism governing droplet breakup and coalescence.

Dilute Water-in-Oil Dispersion. In turbulent flows, the spatial regions where viscous shear is effective are small compared to the size of the large droplets and the dominant external stress is the dynamic pressure of turbulent eddies. In this case, We_{crit} (and the associated maximum drop size, d_{max}) evolves from a balance between the turbulent kinetic energy and the droplet surface energy. In the dilute dispersion Brauner²³ shows that it can be simplified to read:

$$\left(\frac{d_{max}}{D}\right)_{dilute} = 0.55 \left(\frac{\rho_c U_c^2 D}{\sigma}\right)^{-0.6} \left[\frac{\rho_m}{\rho_o(1-\varepsilon_w)} f\right]^{-0.4} \quad (2)$$

Where D is the pipe diameter U_c is the velocity of the continuous (oil) phase, ρ_o , ρ_m and ρ_w denote the densities of oil phase, oil-water mixture and water phase respectively, ε_w is the in-situ water cut and f is the friction factor. The subscript *dilute* denotes the dilute dispersion.

Brauner²³ argued that the drift velocity between water phase and oil phase was negligible at high flow rates. The homogeneous no-slip model is applicable, whereby the in-situ water cut and velocity of the continuous (oil) phase is determined via the superficial water and oil velocities, U_{sw} and U_{so} .

$$\varepsilon_w = \frac{U_{sw}}{U_{sw} + U_{so}}$$

$$U_c = U_{sw} + U_{so} \quad (3)$$

Then, maximum droplet size, d_{max} , in dilute dispersions can be expressed according to Brauner²³ as:

$$\left(\frac{d_{\max}}{D}\right)_{\text{dilute}} = 1.88 \left[\frac{\rho_o (1 - \varepsilon_w)}{\rho_m} \right]^{-0.4} We_o^{-0.6} Re_o^{0.08} \quad (4)$$

Where:

$$Re_o = \frac{\rho_o D U_c^2}{\eta_o} \quad We_o = \frac{\rho_o D U_c^2}{\sigma} \quad f = 0.046 / Re_o^{0.2}$$

It is noted that this equation can be only used in the dilute dispersions i.e. as long as it satisfies the following condition:

$$(1 - \varepsilon_w) \frac{\rho_o}{\rho_m} \cong 1 \quad (5)$$

Dense Water-in-Oil Dispersion. In dense dispersions, droplet coalescence takes place. The previous model is not valid for dense dispersion systems and Brauner²³ extended the Hinze's model to dense dispersion system. Under such conditions, the flow rate of oil phase Q_o should carry sufficient turbulent energy to disrupt the tendency of the water droplets, flowing at a rate Q_w , to coalesce,. Brauner²³ pointed out that the rate of surface energy production in the coalescing water phase is proportional to the rate of turbulent energy supply by the flowing oil phase:

$$\frac{\rho_o U^2}{2} Q_o = C_H \frac{4\sigma}{d_{\max}} Q_w \quad (6)$$

where:

$$Q_o = \frac{\pi}{4} D^2 U_{so}$$

$$Q_w = \frac{\pi}{4} D^2 U_{sw} \quad (7)$$

$$U^2 = 2(ed_{\max})^{2/3}$$

Where C_H is a constant of the order of 1. U' denotes the turbulent kinetic energy.

In the isotropic and homogeneous turbulence, the turbulent kinetic energy can be related to the rate of turbulent energy dissipation, e :

$$e = \frac{4\tau U_o}{D \rho_o (1 - \varepsilon_w)} = \frac{2U_c^3 f}{D} \frac{\rho_m}{\rho_o (1 - \varepsilon_w)} \quad (8)$$

Substituting the equations (7) and (8) into (6) yields

$$\left(\frac{d_{\max}}{D}\right)_{dense} = 2.22C_H^{0.6} \left(\frac{\rho_o U_c^2 D}{\sigma}\right)^{-0.6} \left(\frac{\varepsilon_w}{1-\varepsilon_w}\right)^{0.6} \left[\frac{\rho_m}{\rho_o(1-\varepsilon_w)} f\right]^{-0.4} \quad (9)$$

Where the subscript *dense* denotes the dense oil-water dispersion.

Thus, given a water-oil fluid system and operational conditions, the maximum droplet size that can be sustained is the larger of the two values obtained via (4) and (9), which can be considered as the worst case for a given oil-water system:

$$\frac{d_{\max}}{D} = \text{Max} \left\{ \left(\frac{d_{\max}}{D}\right)_{dilute}, \left(\frac{d_{\max}}{D}\right)_{dense} \right\} \quad (10)$$

Critical Droplet Size

Droplets larger than a critical droplet size d_{crit} separate out from the two-phase flow dispersion either due to *gravity forces*, predominant in horizontal flow, or due to deformation and “*creaming*” typical for vertical flow.²⁵

Gravity effect. Critical droplet diameter d_{cb} above which separation of droplets due to gravity takes place can be found via a balance of gravity and turbulent forces as:²⁵

$$\left(\frac{d_{cb}}{D}\right) = \frac{3}{8} \frac{\rho_o}{|\Delta\rho|} \frac{fU_c^2}{Dg \cos(\theta)} = \frac{3}{8} f \frac{\rho_o}{\Delta\rho} Fr_o \quad (11)$$

Where Froude number is:

$$Fr_o = \frac{U_c^2}{Dg \cos(\theta)}$$

and

$$\Delta\rho = |\rho_o - \rho_w|$$

This effect is predominant at low pipe inclinations i.e. in horizontal and near-horizontal flows.

Creaming. Critical droplet diameter $d_{c\sigma}$ above which drops are deformed and “creamed”, leading to migration of the droplets towards the pipe walls in vertical and near-vertical flows, can be calculated with the equation proposed by Brodkey²⁶:

$$\left(\frac{d_{c\sigma}}{D} \right) = \left[\frac{0.4\sigma}{|\rho_o - \rho_w| g D^2 \cos(\beta)} \right]^{0.5} \quad (12)$$

$$\beta = \begin{cases} |\theta| & |\theta| < 45^\circ \\ 90 - |\theta| & |\theta| > 45^\circ \end{cases}$$

Where θ is the inclination of the pipeline.

The critical diameter, d_{crit} , can then be conservatively estimated for any pipe inclination according to the suggestion made by Barnea²⁵ (1987):

$$\frac{d_{crit}}{D} = Min \left\{ \left(\frac{d_{cb}}{D} \right), \left(\frac{d_{c\sigma}}{D} \right) \right\} \quad (13)$$

Criterion for Stable Water-in-Oil Dispersion

At this point we are in the position to formulate the final criterion for entrainment. The transition from stratified flow to stable water-in-oil dispersion takes places when the oil phase turbulence is intense enough to maintain the water phase broken up into droplets not larger than d_{max} which has to be smaller than the a critical droplet size d_{crit} causing droplet separation. The transition criterion is then (Brauner²³, 2001):

$$d_{max} \leq d_{crit} \quad (14)$$

Introduction of equations (10) and (13) into (14) leads to give us mean to determine the critical velocity.

Water Separation

If the water phase is not entirely entrained and flows separated from oil phase, for corrosion calculations it is crucial to predict the in-situ water cut, water velocity, water film thickness and water wetted pipe cross-section area, in stratified as well as semi-stratified flows.

Stratified Oil-Water Mixture Flow Structure

Neogi et al.²⁷ and Taitel et al.²⁸ proposed a three-layer segregated flow model to calculate the thickness of water layer for gas-water-oil three-phase stratified flow. They considered water, oil and a mixed layer in between as three different “phases” with each phase having its own distinct properties. Also, they proposed that the interfaces between the pure water layer / oil-water mixed layer / pure oil layer are all flat. D. Vedapuri et al.²⁹ used this three-layer segregated flow model to calculate the thickness of water layer and in-situ water cut for oil-water flows. Shi et al.³⁰ proposed a four-layer segregated flow model for calculating in-situ water, water film thickness and water film in-situ velocity

by further dividing the mixed layer into two different layers: water-in-oil and oil-in-water dispersions. They assumed that these two layers are homogeneous and also treated all the interfaces as flat.

It should be pointed out that while appealing, Shi et al.³⁰ four-layer approach gives rise to further difficulties when trying to calculate interfacial shear stresses. Also, from the viewpoint of the corrosion process, water droplets suspended in this mixed layer do not contribute to corrosion and can be ignored. Therefore, in this study, the model is based on a three-layer flow structure (shown in FIGURE 2). All the interfaces are considered to be flat as proposed by Neogi et al.²⁷ and Taitel et al.²⁸.

Momentum Balance

Considering steady state oil-water stratified flow with three-layer flow structure in horizontal pipe flow (shown in FIGURE 3), assuming one-dimensional motion for each layer with no slip between the layers, a momentum balance for each phase yields:

For the pure water layer:

$$-A_w \left(\frac{dp}{dx} \right) - \tau_w S_w - \tau_{i1} S_{i1} = 0 \quad (15)$$

For the oil-water mixed layer:

$$-A_m \left(\frac{dp}{dx} \right) - \tau_m S_m + \tau_{i1} S_{i1} - \tau_{i2} S_{i2} = 0 \quad (16)$$

For the pure oil layer:

$$-A_o \left(\frac{dp}{dx} \right) - \tau_o S_o + \tau_{i2} S_{i2} = 0 \quad (17)$$

Where the subscripts w , m and o denote the water layer, the oil-water mixed layer, and the pure oil layer, respectively. The subscripts of $i1$ and $i2$ represent the interfaces of pure water layer/oil-water mixed layer and oil-water mixed layer / pure oil layer, respectively, τ denotes shear stress, S represents the wetted perimeters by each of the layers, dp/dx denotes the pressure gradient, A_w , A_m and A_o denote the cross sectional areas occupied by the water phase, oil-water mixture and oil phase respectively.

Since the pressure gradient dp/dx is same in the three layers³¹, we can combine the equations(15), (16) and (17) to eliminate it. The following two equations can be derived:

$$\tau_o \frac{S_o}{A_o} - \tau_m \frac{S_m}{A_m} - \tau_{i1} \frac{S_{i1}}{A_m} + \tau_{i2} \left(\frac{S_{i2}}{A_o} + \frac{S_{i2}}{A_m} \right) = 0 \quad (18)$$

$$\tau_m \frac{S_m}{A_m} - \tau_w \frac{S_w}{A_w} - \tau_{i2} \frac{S_{i2}}{A_m} + \tau_{i1} \left(\frac{S_{i1}}{A_w} + \frac{S_{i1}}{A_m} \right) = 0 \quad (19)$$

All the shear stresses can be evaluated by using *Blasius* type equation (Taitel and Dukler³¹, 1976) with all the friction factors evaluated using the approach similar to the one proposed by Brauner³² (1989).

Mass Balance

Based on the three-layer oil-water flow structure (shown in FIGURE 3) discussed above a mass balance for each phase is:

$$Q_W = Q_{WL} + \varepsilon_M Q_M \quad (20)$$

$$Q_O = Q_{OL} + (1 - \varepsilon_M) Q_M \quad (21)$$

Where Q_W , and Q_O denote the total input volume flow rates of water phase and oil phase. Q_{WL} , Q_{OL} and Q_M represent the flow rates of pure water layer, pure oil layer and oil-water mixed layer. ε_M denotes the water cut in the oil-water mixed layer.

Equations (20) and (21) can be divided by the pipe cross section area to give the superficial velocity of for each layer:

$$U_{SW} = U_{SWL} + \varepsilon_M U_{SM} \quad (22)$$

$$U_{SO} = U_{SOL} + (1 - \varepsilon_M) U_{SM} \quad (23)$$

Here U_{SW} is the total superficial water velocity, U_{SWL} is the superficial velocity for the water phase flowing in the pure layer while $\varepsilon_M U_{SM}$ is the superficial velocity for the water phase flowing in the mixed layer. Similarly U_{SO} , U_{SOL} and $(1 - \varepsilon_M) U_{SM}$ represent the corresponding superficial oil velocities. ε_M denotes the water cut in the mixed layer.

To solve the momentum and the mass balance equations (18, 19, 20 and 21) simultaneously, the number of equations must be equal to the number of unknowns. However, we have six unknowns: U_{SWL} , U_{SOL} , U_{SM} , A_W , A_M and ε_m . Hence, we need two more equations.

A new method is proposed here to calculate the superficial velocity U_{SM} of oil-water mixture layer. From the discussion of water entrainment in the previous section, we can postulate that the entrainment factor, FE of the water phase by flowing oil phase is proportional to the magnitude of the oil velocity with respect to the critical velocity required for total entrainment, i.e. the closer we are to the critical velocity, the more water is entrained. Therefore we can write:

$$FE = \left(\frac{U_{SO}}{U_{crit}} \right)^a \quad (24)$$

Where a is a constant of the order of one. U_{SO} denotes the superficial oil velocity.

By simple manipulation, the superficial velocity U_{SWL} of pure water layer can be calculated as the following formula:

$$U_{SWL} = U_{SW} (1 - FE) \quad (25)$$

In the present stage of model development, the water cut in the oil-water mixture layer, ε_m , has been assumed to be 50% (without having other means of estimating it). Based on this assumption, the total superficial velocity of oil-water mixed layer can be obtained:

$$U_{SM} = 2 U_{SW} FE \quad (26)$$

Hence, the superficial velocity of pure oil layer can be calculated with the following equation:

$$U_{SOL} = U_{SO} - U_{SW} FE \quad (27)$$

Solution Procedure

The fluid properties of oil and water phases, such density and viscosity, and the total mixture velocity of oil and water and the water cut are the user's inputs as well as the pipe diameter and inclination. The input superficial oil and water velocities, U_{SW} and U_{SO} , are then calculated. The water cut ε_m in the oil-water mixed layer is set to 50%. Hence, the superficial velocities of pure water layer, oil-water mixed layer and pure oil layer are calculated with the equations (25), (26) and (27). At this point, the combined momentum equations (18) and (19) are solved to predict the cross sectional areas occupied by the water phase A_W and oil-water mixture A_M enabling us to via simple geometrical calculations obtain film heights h_W and h_L (shown in FIGURE 3). Once the film thickness is calculated, the in-situ velocities (U_W , U_M and U_O) of the three layers can be obtained.

RESULTS AND DISCUSSION

Experimental Validation

A comparison between the experimental results and predictions made by the water entrainment model for different flow regimes was done. All the experimental results were obtained from Shi et al.³⁰, Trallero et al.¹⁶, Nadler and Mewes¹⁸ and Angeli and Hewitt¹⁹. TABLE 1 summarizes the important parameters in their experiments.

The model predicts the experimentally observed *stratified flow* pattern with an accuracy of 80% (40 out of 50 cases). For *water-in-oil dispersed flow* a somewhat weaker agreement between the predictions and experimental data is seen with an agreement of 70% (35 out of the 50 cases simulated). Given the uncertainty in the experimental results as well as the arbitrariness of some of the constants used in this first version of the water entrainment model the agreement can be considered as reasonable. When compared with this pool of cases, other models and rules of thumb listed in the literature review above predict with accuracy just above 50%.

Comparisons were made between the predicted results by the three-layer model described above and experimental data for the pure water layer thickness (taken from the water/oil flow measurements of Shi et al.³⁰) at input water cuts of 20% and 40%. All the experiments were conducted at 25°C in a 200'

long, 4" ID multiphase flow loop at Ohio University. The properties of LVT200 oil used at 25°C were: $\rho_o=820 \text{ kg/m}^3$, $\mu_o=2 \text{ cP}$. The ASTM seawater was used with the following properties: $\rho_w=1024 \text{ kg/m}^3$, $\mu_w=1 \text{ cP}$. Oil water surface tension was $\sigma =0.029 \text{ N/m}$. The oil-water mixture velocity flow rate was in the range of 0.4 - 3.0 m/s. From the comparison, shown in FIGURE 4 and FIGURE 5 it is found that the largest discrepancy exists for the lower water cut (20%) at low velocities. At the higher water cut (40%) and higher flow rate a reasonable agreement between the experimental and the predicted data is achieved. The reasons for this performance are being currently investigated and it appears that more accurate experimental data are needed to calibrate and improve the existing model.

Parametric Testing of the Model for Critical Entrainment Velocity

FIGURE 6 shows the effect of water cut on critical velocity for a test case $\rho_o=820 \text{ kg/m}^3$, $\mu_o=2 \text{ cP}$ $D=0.1 \text{ m}$ and $\sigma=0.029 \text{ N/m}$ corresponding to a light crude oil with API around 41. Increasing water cut leads to higher critical velocity of flowing oil phase required for entrainment. Water cut significantly affects the critical velocity and the commonly used 1 m/s threshold is recovered for very low water cuts. It is noted that the curve in FIGURE 6 is valid only for the particular combination of parameters listed there and the actual numbers change when any of the parameters is modified, however, without changing the character of the overall dependence. This holds of all of the simulations discussed below.

FIGURE 7 shows the effect the pipe diameter on the critical velocity. Again the common 1 m/s cutoff velocity is recovered for 10 cm ID pipe, however the threshold increases significantly with pipe diameter and almost doubles for a 50 cm ID pipe. This point highlights the error made when results from small diameter pipes are simply scaled up.

The effect of oil density on the critical velocity is shown in FIGURE 8. Increasing oil density significantly decreases the critical velocity. As the oil density approaches that of water, the miscibility between oil and water increases. The momentum and mass exchange between them is much easier, i.e. water can be much easier entrained and suspended by a heavy oil phase.

FIGURE 9 shows the effects of oil surface tension on the critical velocity. Increasing oil surface tension by adding surfactants will only slightly increase the critical velocity. High surface tension corresponds to high surface energy of droplets. This means that higher turbulent kinetic energy, which is proportional to high flow rate of the flowing oil phase, is needed to deform and break the droplets.

The effect of oil viscosity shown in FIGURE 10 is relatively small. The oils with high viscosities have a slightly higher tendency to form stable oil-water emulsion. Once water droplets are entrained in the flowing oil phase, they will be stabilized and suspended as droplets in the oil phase because the coalescence of droplets decreases with increasing the oil viscosity. In this case, lower coalescence at higher oil viscosity leads to a lower critical velocity to form stable water-in-oil dispersion.

CONCLUSION

- In this study, a newly published method is used to predict the critical velocity for entraining free water by the flowing oil phase.

- For stratified flow, a new model is proposed to predict the thickness of pure water layer and in-situ water layer velocity, which are crucial for corrosion calculation.
- The two models were compared with available experimental results with moderate success. New more extensive and accurate experiments are needed before any further improvements of the model can be made.

ACKNOWLEDGEMENT

The authors would like to acknowledge the contribution of the consortium of companies whose continuous financial support and technical guidance led to the publishing of this work. They are BP, ConocoPhillips, ENI, Petrobras, Saudi Aramco, Shell, Total, Champion Technologies, Clariant, MI Technologies and Nalco. The authors are grateful to the Russ College of Engineering and Technology for providing logistical support for C. deWaard's visit to Ohio University.

REFERENCE

- 1 Wicks, M., and Fraser, J.P., "Entrainment Of Water By Flowing Oil", *Materials Performance*, May 1975, pp. 9~12.
- 2 Wu, Y., "Entrainment Method Enhanced to Account fro Oil's Water Content", *Oil & Gas Technology*, Aug. 28, 1995, pp. 83~86.
- 3 L.M.Smith, M.J.J. Simon Thomas and C. de Waard, "Controlling Factors in the Rate of CO₂ Corrosion", UK. Corr.'87 Brighton, 26-28 Oct., 1987
- 4 C. de Waard and U. Lotz, "Prediction of CO₂ Corrosion of Carbon Steel", *Corrosion/93*, paper no. 69, (Houston, TX: NACE International, 1993)
- 5 C. D. Adams, J. D. Garber, F. H. Walters, C. Singh, "Verification of Computer Modeled Tubing Life Predictions by Field Data", *Corrosion/93*, paper no. 82, (Houston, TX: NACE International, 1993)
- 6 C.de Waard, L.Smith and B.D. Craig, "The Influent of Crude Oil on Well Tubing Corrosion Rates", *EUROCORR 2001*
- 7 Russell, T. W. F., Hodgson, G.W., and Govier, G. W., "Horizontal Pipelines Flow of Mixtures of Oil and Water", *Can. J. of ChE*, **37**, 9-17, 1959
- 8 Charles, M.E., Govier, G.W. and Hodgson, G.W., "The Horizontal Pipelines Flow of Equal Density Oil-water Mixture", *Can. J. Chem. Eng.*, **39**, 27-36, 1961
- 9 Ward, J.P. and Knudsen, J.G, "Turbulent Flow of Unstable Liquid-Liquid Dispersions: Drop Size and Velocity Distributions", *AIChE. J.*, **13**, No 2, 356-367, 1967

- 10 Oglesby, K. D., "An Experimental Study on the Effects of Oil Viscosity, Mixture Velocity and Water Fraction on Horizontal Oil-Water flow", M.S. Thesis, University of Tulsa, 1979
- 11 Mukherjee, H., Brill, J.P., and Beggs, H. D., "Experimental Study of Oil-Water Flow in Inclined Pipes", *J. of Energy Resources Technology*, 56-66, March, 1981
- 12 Arirachakaran, S., K. D., Oglesby, M. S., Malinovsky, M.S., Shoham, O., and J.P. Brill, "An Analysis of Oil-Water Flow Phenomena in Horizontal Pipes", *SPE* paper 18836, 155-167, 1989
- 13 Pal, R., "Pipeline Flow of Unstable and Surfactant-Stabilized Emulsions", *AIChE J.*, **39**, No.11, 1754-1764, 1993
- 14 Pal, R., "Effect of Droplet Size on the Rheology of Emulsions", *AIChE J.*, **42**, No.11, 3181-3190, 1996
- 15 Kurban, A. P. A., Angeli, P. A., Mendes-tatsis, M. A., and Hewitt, G. F., "Stratified and Dispersed Oil-Water Flows in Horizontal Pipes", *Multiphase 95*, 277-291, 1995
- 16 Trallero, J. L, Sarica, C and J. P. Brill, "A Study of Oil-Water Flow Patterns in Horizontal Pipes", *SPE*, Paper No. 36609, 363-375, 1996
- 17 Flores, J. G., Sarica, C., Chen, T. X., and Brill, J. P., "Investigation of Holdup and Pressure Drop Behavior for Oil-Water Flow in Vertical and Deviated Wells", *ETCE-98*, Paper No. 10797, 1997
- 18 Nadler, M. and Mewes, D, "Flow Induced Emulsification in the Flow of Two Immiscible Liquids in Horizontal Pipes", *Int. J. Multiphase Flow*, **23**, 56-68, 1997
- 19 Angeli, P., and Hewitt, G. F, "Drop Size Distributions in Horizontal Oil-Water Dispersed Flows", *Chem. Eng. Sci.* **55**, 3133-3143, 2000
- 20 Corlett, A.E., and Hall, A.R.W., "Viscosity of Oil and Water Mixtures", *Multiphase 99*, 595-603, 1999
- 21 H.Shi, "A Study of Oil-Water Flows in Large Diameter Horizontal Pipelines", Ph.D Dissertation, Ohio University, 2001
- 22 Brauner, N., Moalem Maron, "Flow Pattern Transitions in Two-phase Liquid-liquid Horizontal Tubes", *Int. J. of Multiphase Flow*, Vol.18, pp. 123~140(1992a).
- 23 Brauner, N., "The Prediction of Dispersed Flows Boundaries in Liquid-Liquid and Gas-liquid Systems", *Int. J. of Multiphase Flow*, Vol.27, pp. 885~910(2001)
- 24 Hinze, J., "Fundamentals of the Hydrodynamic Mechanism of Splitting in Dispersion Process", *AIChE*, Vol. 1(1955), No. 3, pp. 289~295
- 25 Barnea, D., "A Unified Model for Predicting Flow Pattern Transitions for the Whole Range of Pipe Inclinations", *Int. J. of Multiphase Flow*, Vol.11, pp. 1~12(1987)
- 26 Brodkey, R.S., "The Phenomena of Fluid Motions", Addison-Wesley, Reading, M.A., 1969

- 27 Neogi, S., Lee, A.H. and Jepson, W.P., “A Model for Multiphase (Gas-Water-Oil) Stratified Flow in Horizontal Pipelines”, SPE 28799, pp.553-561,1994
- 28 Taitel, Y., Barnea, D. and Brill, J.P., “Stratified Three-phase Flow in Pipes”, Int. J. Multiphase Flow, Vol. 21, No.1, pp. 53-60,1995
- 29 D. Vedapuri, D. Bessette and W.P. Jepson, “A Segregated Flow Model to Predict Water Layer Thickness in Oil-Water Flows in Horizontal and Slightly Inclined Pipelines”, Multiphase’97, pp. 75-105.
- 30 Hua Shi, Hongbin Wang and W.P. Jepson, “Prediction of water Film Thickness and Velocity for Corrosion Rate Calculation in Oil-Water Flows”, NACE 2002, Paper No.02500, pp. 1-18, 2002
- 31 Taitel, Y. and Dukler, A.E., “A Model for Predicting Flow Regime Transitions in Horizontal and Near Horizontal Gas Liquid Flow”, AIChE J., Vol.22, No.1, pp.47, 1976
- 32 N. Brauner and Maron, D.M., “Two-phase Liquid-liquid Stratified Flow”, Physicochemical Hydrodynamics, Vol. 11, No.4, pp.487-506, 1989.

TABLE 1. Summary of the experimental parameters in the studies used for verification

Reference	D (cm)	ρ_o (kg/m ³)	ρ_w (kg/m ³)	μ_o (cP)	μ_w (cP)	σ (N/m)	θ (°)	T (°C)	ε_w (%)	Mixture velocity (m/s)
30	10	820	1024	2	1	0.029	0	25	20-40	0.4-3.0
16	5.08	850	1000	29.6	1	0.036	0	20	10-90	0.5-3.0
19	2.5-7.6	801	1000	1.6	1	0.017	0	20	20-80	0.7-3.9
18	5.9	790	1000	22-35	1	0.036	0	18-30	10-20	0.1-2.0

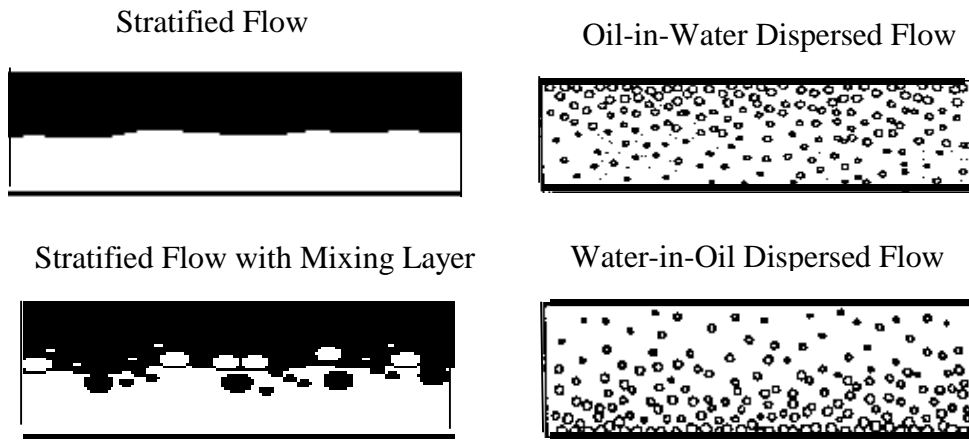


FIGURE 1. Flow patterns in oil-water horizontal flows

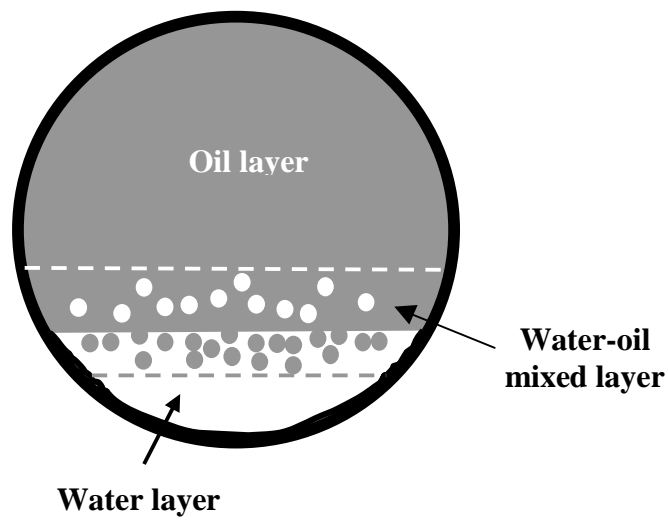


FIGURE 2. Cross-section for a three-layer flow structure with a planar interface

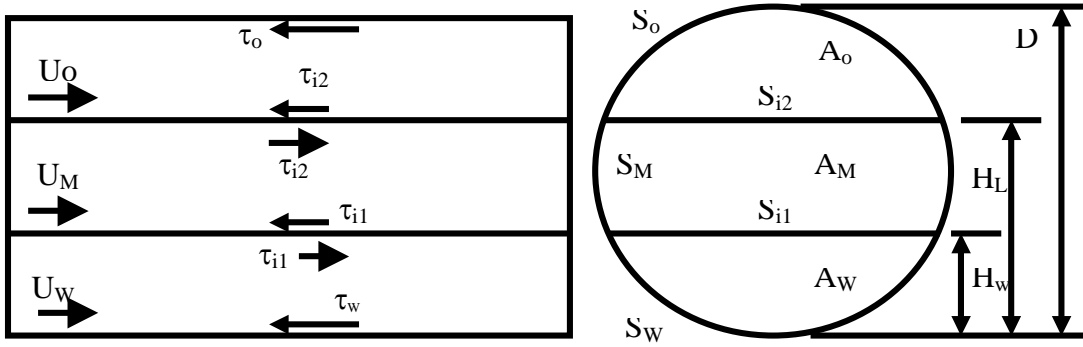


FIGURE 3. Schematic representation of the three-layer segregated oil-water flow

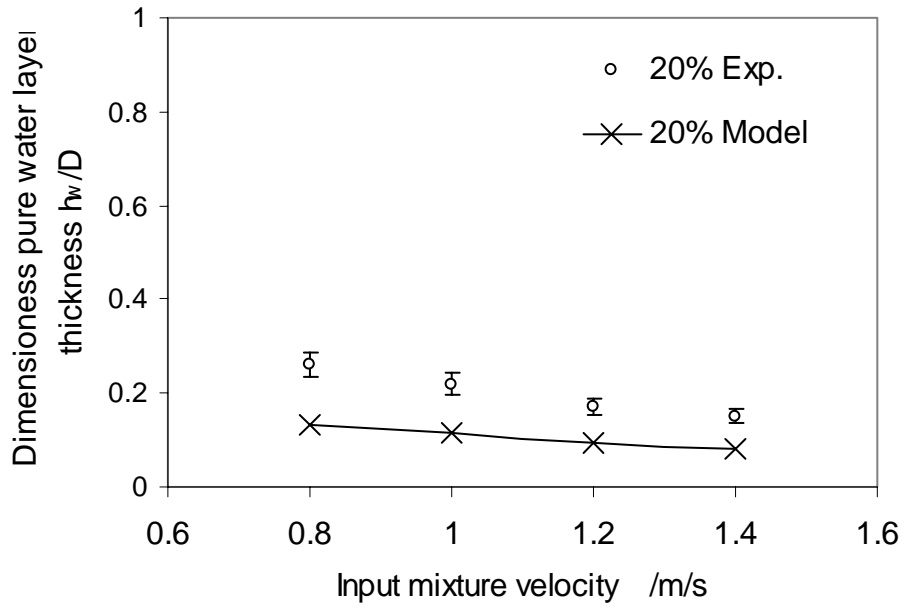


FIGURE 4. Comparison between the predicted results by the model and experimental data of pure water layer thickness (Shi et al.³⁰) at input water cut of 20%.

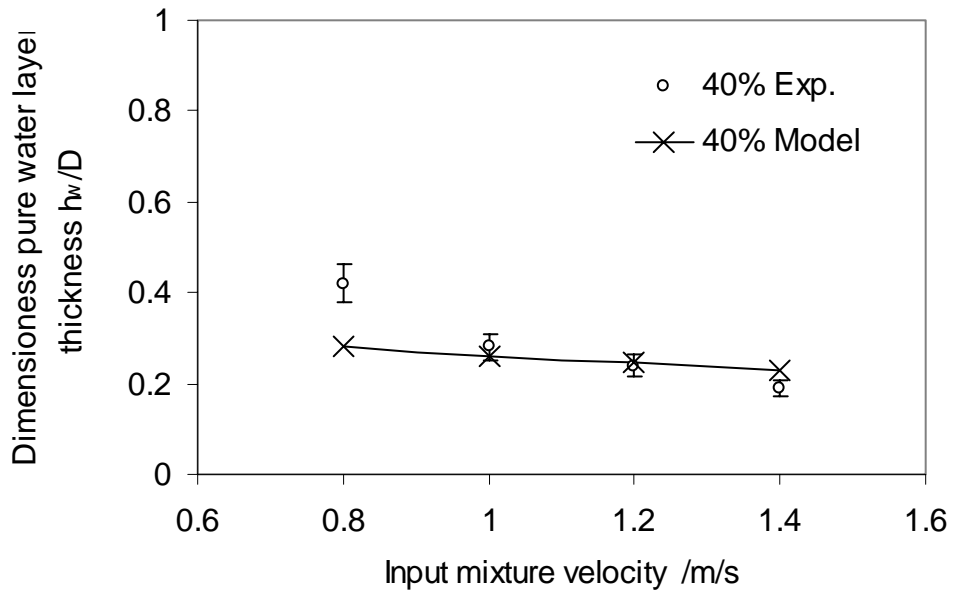


FIGURE 5. Comparison between the predicted results by the model and experimental data of pure water layer thickness (Shi et al.³⁰) at input water cut of 40%.

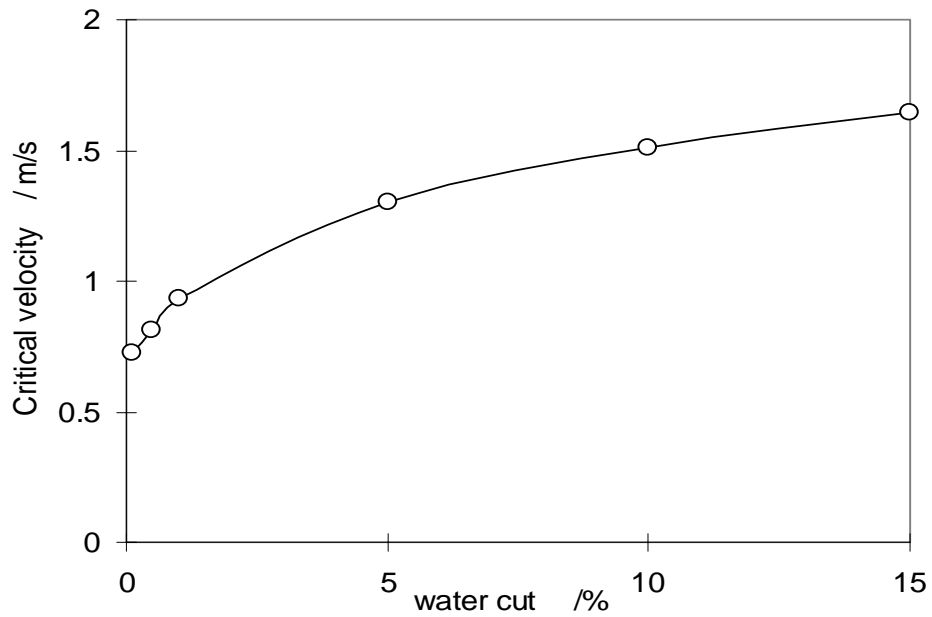


FIGURE 6. Effect of water cut on critical velocity at $\rho_o=820 \text{ kg/m}^3$, $\mu_o=2 \text{ cP}$
 $d=0.1 \text{ m}$ and $\sigma=0.029 \text{ N/m}$

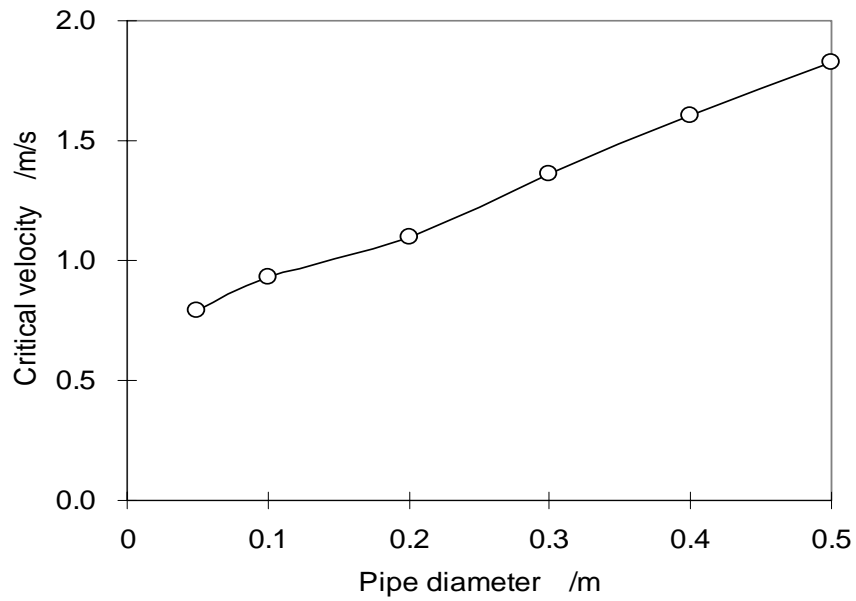


FIGURE 7. Effect of pipe diameter on critical velocity at $\rho_o=820 \text{ kg/m}^3$, $\mu_o=2 \text{ cP}$, water cut=1% and $\sigma=0.029 \text{ N/m}$

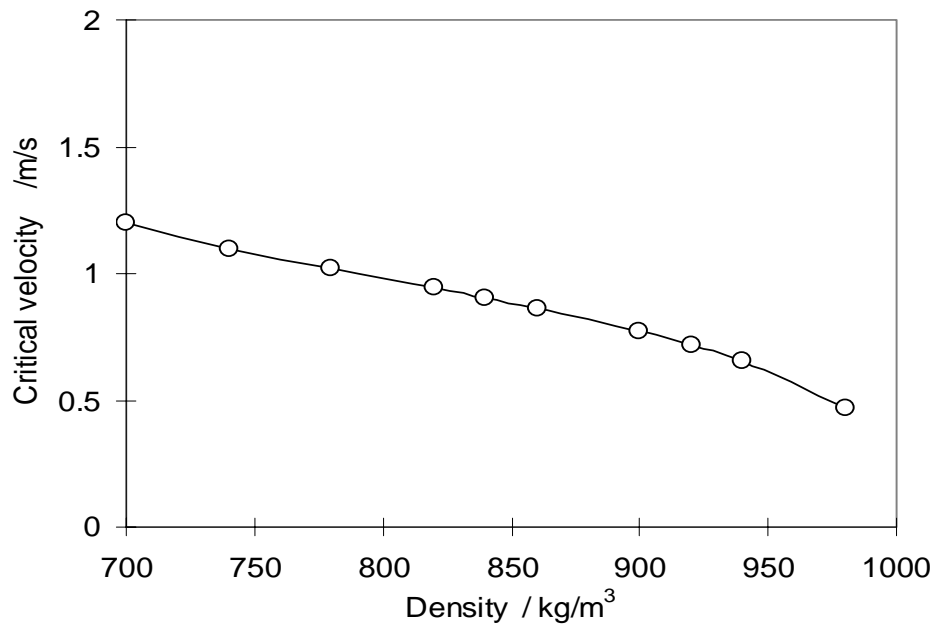


FIGURE 8. Effect of oil density on critical velocity at $D=0.1 \text{ m}$, $\mu_o=2 \text{ cP}$, water cut=1% and $\sigma=0.029 \text{ N/m}$

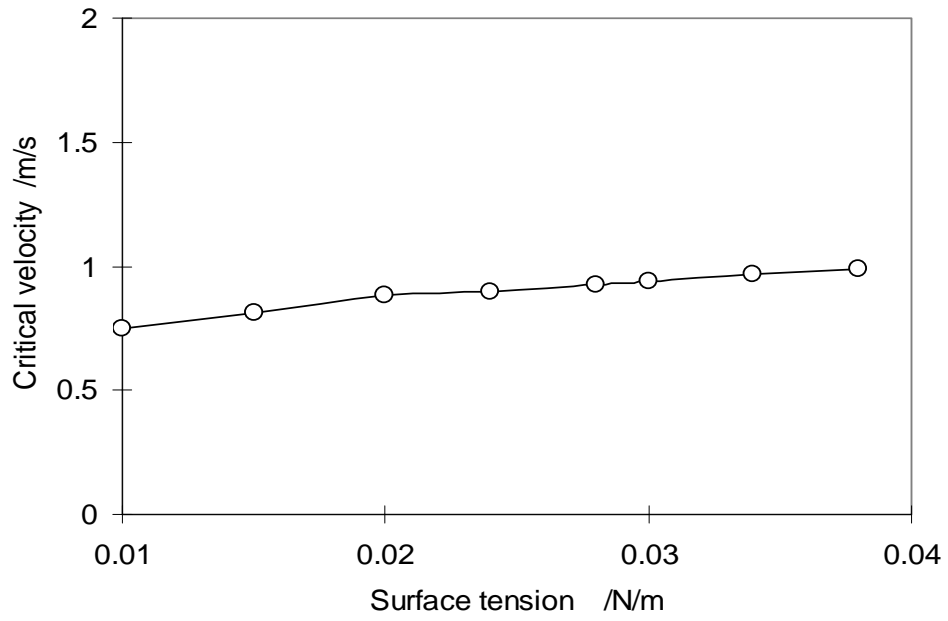


FIGURE 9. Effect of surface tension on critical velocity at $D=0.1$ m, $\mu_o=2$ cP, water cut=1% and $\rho_o=820$ kg/m³

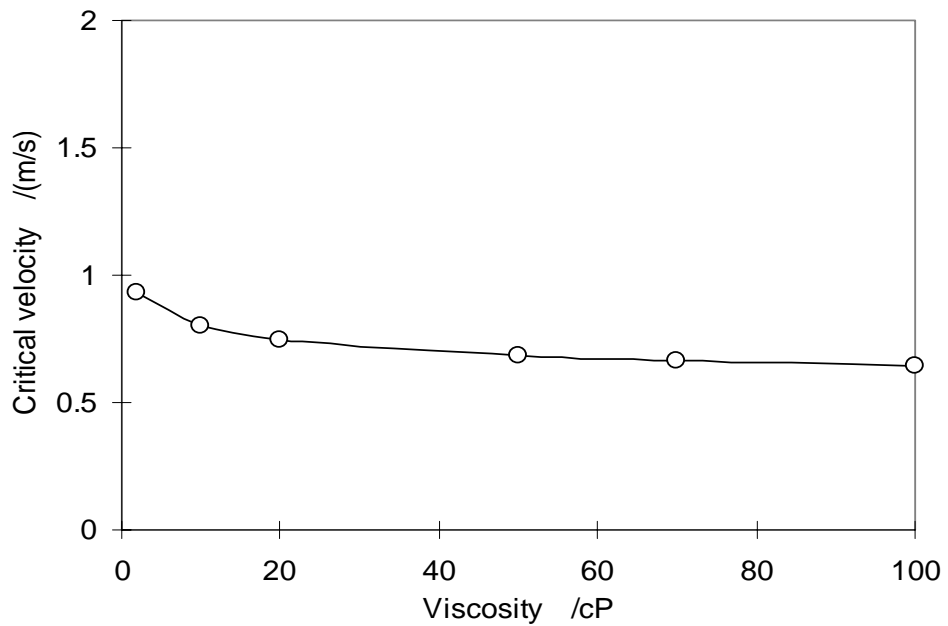


FIGURE 10. Effect of viscosity on critical velocity at $D=0.1$ m, $\sigma=0.029$ N/m, water cut=1% and $\rho_o=820$ kg/m³